Positron-annihilation study of vacancy defects in InAs

J. Mahony and P. Mascher
Department of Engineering Physics, McMaster University, Hamilton, Ontario, Canada L8S 4L7
(Received 16 September 1996)

Positron lifetime measurements on InAs wafers have shown that the positron bulk lifetime in InAs is 246 ± 2 ps. Most samples exhibit a defect lifetime of 287 ± 6 ps, which is attributable to monovacancy-impurity complexes with a concentration of $7\pm2\times10^{16}$ cm^{-3}. Very heavily doped *n*-type samples exhibit a defect lifetime of 332–340 ps. The defects in these samples have divacancy character, but change their configuration at low temperatures to a monovacancy-type defect. The concentration of these defects is also close to 10^{17} cm^{-3}. Both types of defects are stable for rapid thermal annealing up to 850 °C, and both defects are neutral. It is proposed that the formation of the divacancy-type defects may be correlated with a discrepancy between the carrier concentration and the total dopant concentration. [S0163-1829(97)07115-4]

I. INTRODUCTION

InAs is a high-mobility, narrow-band-gap semiconductor that is suitable for many different electrical and far-infrared optical applications, including heterojunction field-effect transistors,[1] resonant-tunneling diodes,[2] bipolar transistors,[3] and far-infrared lasers.[4] Compared to more common III-V semiconductors such as GaAs and InP, however, very little is known about the point defect characteristics of InAs.

Positron lifetime spectroscopy (PLS) is an effective tool for characterizing vacancy-type defects in III-V compound semiconductors. Lifetimes that result from annihilations of positrons in trapped defect states can indicate the size of the open volume of the defect when compared to the lifetime for annihilations in the delocalized Bloch state, often called the ''bulk lifetime.'' To use PLS as a defect characterization tool, it is therefore crucial that the bulk lifetime of the material be accurately known. There are several reported results of positron lifetime measurements in InAs; however, the bulk lifetime values vary significantly. Dannefaer[5] reported a bulk lifetime of 247 ps for InAs, although no defect-related lifetime components were resolved. Brudnyi, Vorobiev, and Tsoi[6] found a lifetime of 285 ps, and suggested that this corresponds to the bulk lifetime of InAs. Dlubek and Brümmer[7] measured a single polycrystalline sample of InAs, found average lifetimes of 260 and 255 ps before and after annealing, respectively, and concluded that the bulk lifetime of InAs was 257 ± 3 ps. Misheva *et al.*[8] reported a bulk lifetime of 274 ± 1 ps, and a defect lifetime of 416 ± 7 ps which was attributed to divacancies. Liszkay, Bottyán, and Balogh[4] reported an average lifetime of 213 ps in as-grown material, increasing to 230 ps after electron irradiation to a fluence of 3×10^{18} cm^{-2}. Due to the significant scatter in reported bulk lifetime values, PLS at this point has not contributed reliable information about the defect characteristics of InAs.

In this paper, PLS measurements on a large number of variously doped single crystalline InAs wafers are described. The purpose of this study is twofold: First, to determine the bulk and defect positron lifetimes in InAs accurately, and second, to investigate the doping dependence of the defect characteristics.

II. EXPERIMENTAL DETAILS

The InAs samples were cleaved from polished wafers cut from single crystals grown at the Institute of Electronic Materials Technology in Warsaw, Poland, and contained a wide range of dopant concentrations. Carrier concentrations and mobilities were measured using the Hall effect. Etch pits were revealed on ⟨111⟩-oriented crystals using a solution of $0.4N$ Fe^{3+} in HCl at 25 °C,[10] and etch pit densities (EPD's) were measured using an optical microscope. The EPD's range from mid-10^3 to low-10^5 cm^{-2} (Tables I and II), consistent with device grade wafer material. The temperature stability of the measured defect characteristics was tested using rapid thermal annealing, performed in flowing nitrogen for 10 s with a temperature ramp of 100 °C/s. This procedure is consistent with conventional wafer treatment for device applications and avoids the use of As overpressures, which would be necessary in prolonged annealing studies due to the relatively low congruent sublimation temperature of InAs [380 °C (Ref. 11)].

Positron lifetime spectroscopy was performed using three different spectrometers with time resolutions [full width at half maximum (FWHM)] of between 205 and 230 ps, and channel widths of approximately 19 ps. The positron sources were ^{22}NaCl encapsulated in Al foil of thickness 0.65 mg/cm^2, and had activities between 10 and 20 μCi, yielding peak to background ratios of 3×10^3–7×10^3. To account for annihilations in the Al foil, lifetimes of 155 and 256 ps with absolute intensities of 1.60% and 4.12% were subtracted from the spectra.

The positron lifetime spectra were analyzed using PATFIT88.[12] At least two spectra were measured for each sample condition. Measurements were made as a function of the spectrum area to determine the minimum number of lifetimes required to obtain a good fit. For two-lifetime fits, good χ-squared values were only possible for spectrum areas less than approximately 2×10^6. As was previously observed in InP,[13] two-lifetime fits became statistically unacceptable for larger spectrum areas. Three-lifetime fits yielded good χ-squared values for all spectra, some with areas as large as 3×10^7 counts. However, an area of 7×10^6 counts was sufficient to obtain consistent results, and this spectrum area

TABLE I. Physical characteristics and room-temperature positron lifetime parameters for several InAs wafers. The values are determined from the average of several spectra. The uncertainties represent the standard deviation in repeated measurements.

Sample I.D.	Dopant	Carrier type	Carrier density (cm^{-3})	Mobility ($cm^2/V\,s$)	Orientation	EPD (cm^{-2})	τ_1 (ps)	τ_2 (ps)	I_2 (%)	τ_B^{TM} (ps)	τ_{AVG} (ps)	κ (ns^{-1})
1	Zn	*p*	2.2×10^{18}	140	⟨111⟩	1×10^5	199±23	282±12	61±17	245±2	251±1	0.9±0.4
2	Zn	*p*	4.5×10^{17}	180	⟨111⟩	2×10^5	200±22	280±11	62±17	245±2	251±1	0.9±0.4
3	Zn	*p*	1.9×10^{17}	180	⟨111⟩	1×10^5	208±23	286±14	54±21	247±2	252±1	0.8±0.5
4	none	*n*	6.4×10^{14}	8500	⟨111⟩	2×10^4	213±8	290±8	49±10	245±1	251±1	0.6±0.2
5	none	*n*	7.0×10^{14}	9400	⟨111⟩	4×10^4	210±6	285±5	55±7	245±1	251±1	0.6±0.2
6	none	*n*	8.0×10^{14}	10 000	⟨111⟩	5×10^4	211±11	287±9	53±12	245±2	251±1	0.7±0.2
7	none	*n*	4.0×10^{16}	18 000	⟨111⟩	4×10^4	195±18	279±7	64±10	242±5	249±3	0.9±0.3
8	none	*n*	4.8×10^{16}	18 000	⟨100⟩		199±12	286±6	60±8	244±3	252±2	0.9±0.2
9	Se	*n*	7.3×10^{16}	21 000	⟨111⟩	1×10^4	216±9	289±12	50±14	247±1	252±1	0.6±0.2
10	Se	*n*	7.6×10^{17}	14 000	⟨111⟩	2×10^5	215±9	292±10	48±12	246±2	251±1	0.6±0.2
11	Se	*n*	9.0×10^{17}	13 000	⟨111⟩	6×10^4	220±7	299±13	41±12	246±1	251±1	0.5±0.2
12	Sn	*n*	3.0×10^{18}	8200	⟨111⟩	3×10^5	219±3	293±3	44±3	246±1	251±1	0.5±0.1
13	S	*n*	5.0×10^{18}	7000	⟨100⟩		215±19	292±13	48±19	246±3	252±2	0.6±0.3

was used for the measurements reported in this study. The longest lifetime τ_3 was essentially constant at 1.7 ns, with an intensity of approximately 0.1%. This component is likely due to annihilations in the ^{22}NaCl, and was therefore removed from the spectra.

III. RESULTS

Table I shows the physical characteristics and the positron lifetime parameters for several *p*- and *n*-type InAs wafers. τ_1, τ_2, and I_2 are parameters fit to the lifetime spectra, where τ_2 corresponds to the lifetime of positrons trapped at a defect, and I_2 is the corresponding intensity. τ_B^{TM} is the bulk lifetime of positrons calculated from the fit parameters using the conventional trapping model,[14] and should equal the actual bulk lifetime τ_B when this model is valid. For every sample, τ_B^{TM} is constant at 246±2 ps. The current value is in excellent agreement with that of 247 ps reported by Dannefaer.[5] Therefore, we will adopt the value of 246±2 ps for the bulk lifetime of positrons in InAs.

τ_{AVG} is the average lifetime of positrons in the sample, a parameter often used to monitor qualitative changes in the lifetime spectra. The trapping rate of positrons into the defects κ is proportional to the concentration of positron traps, and has been calculated using the conventional trapping model. The equations relating the various parameters are

$$\tau_B^{TM}=\left[\frac{I_1}{\tau_1}+\frac{I_2}{\tau_2}\right]^{-1}, \tag{1}$$

$$\tau_{AVG}=I_1\tau_1+I_2\tau_2, \tag{2}$$

$$\kappa=\frac{I_2}{I_1}\left[\frac{1}{\tau_B}-\frac{1}{\tau_2}\right], \tag{3}$$

where $I_1=1-I_2$.

The samples in Table I all show very similar positron lifetime characteristics, with a defect-related lifetime component of 287±6 ps. The defect lifetime may be slightly shorter than the average in the *p*-type samples, and slightly longer than the average in the Se-, S-, and Sn-doped samples; however, this apparent trend toward a longer defect lifetime in *n*-type samples is obscured by the uncertainty in the measurements. The trapping rate into the defects exhibiting the 287-ps lifetime is 0.7±0.2 ns^{-1}.

The very heavily S- and Sn-doped wafers (Table II) show markedly different positron lifetime characteristics. In these samples, the defect lifetime is much longer at 332–340 ps, with a trapping rate of approximately 0.7 ns^{-1}. The average lifetime is longer by about 8 ps in these samples compared to those in Table I; however, the bulk lifetime is consistent, indicating that the standard trapping model is also valid in the heavily doped samples.

TABLE II. Physical characteristics and room-temperature positron lifetime parameters for heavily doped *n*-type InAs:(S+Sn) wafers. The values are determined from the average of several spectra. The uncertainties represent the standard deviation in repeated measurements.

Sample I.D.	Carrier density (cm^{-3})	Mobility ($cm^2/V\,s$)	Orientation	EPD (cm^{-2})	τ_1 (ps)	τ_2 (ps)	I_2 (%)	τ_B^{TM} (ps)	τ_{AVG} (ps)	κ (ns^{-1})
14	4.2×10^{19}	2100	⟨111⟩	4×10^3	214±3	340±6	36±3	247±2	260±2	0.6±0.1
15	4.2×10^{19}	1800	⟨111⟩	5×10^3	210±2	332±3	39±2	245±1	257±1	0.7±0.1
16	5.9×10^{19}	1500	⟨111⟩	1×10^4	212±5	340±6	38±4	247±1	260±2	0.7±0.1

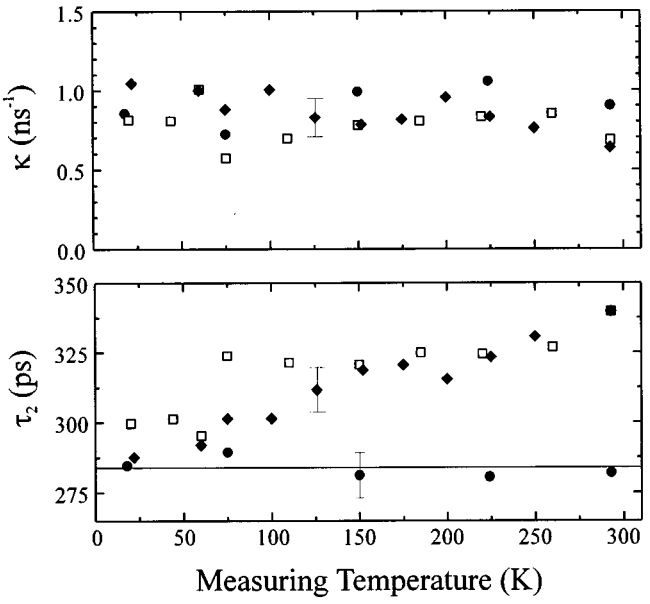

FIG. 1. Defect lifetime τ_2 and trapping rate κ as functions of measuring temperature for samples 1 (●), 14 (♦), and 16 (□).

PLS measurements were made at temperatures down to 25 K for samples 1, 8, 14, and 16. For all samples, τ_B^{TM} was constant, allowing the standard trapping model to be used to calculate the trapping rates. The results for samples 1, 14, and 16 are shown in Fig. 1. Sample 1 showed no temperature dependence of the positron lifetime characteristics, as was the case for sample 8. However, for samples 14 and 16 a significant temperature effect is observed. The defect lifetime undergoes a gradual transition from ~340 to ~290 ps in sample 14, and ~300 ps in sample 16. The trapping rates for samples 14 and 16 do not show any significant temperature dependence.

Rapid thermal annealing up to 850 °C was performed on samples 1, 3, 6, 7, 9, 11, 13, 14, and 16. In all of these samples, the positron lifetime characteristics did not change appreciably, indicating that the defects which exhibit the 287-ps positron lifetime and those exhibiting the 340-ps lifetime did not anneal out, even at temperatures well above that for congruent sublimation.

IV. DISCUSSION

The defect lifetime of 287 ± 6 ps observed in samples 1–13 likely originates from a defect that has an open volume comparable to a monovacancy, based on the ratio $\tau_2/\tau_B=1.17$. Theoretical calculations of the positron lifetimes for vacancies on the As and In sublattices yielded values of 299 and 285 ps, respectively.[15] While the theoretical lifetime for V_{As} is closer to the present experimental value, the inherent uncertainty in the calculation and the fact that lattice relaxations were not taken into account do not allow a definitive identification of the sublattice on which the monovacancy resides. In addition, the lifetime may be slightly altered if the monovacancies are complexed.

Theoretical calculations for the ionization levels of vacancies in InAs have predicted that V_{As} is always positive, and that V_{In} has $(0/-)$, $(-/2-)$, and $(2-/3-)$ levels at $E_v+0.10$ eV, $E_v+0.13$ eV, and $E_v+0.23$ eV, respectively.[16] The fact that the trapping rate into the defects exhibiting the 287-ps lifetime does not change with temperature indicates that the defects are neutral[17] for a wide range of Fermi levels. It is therefore unlikely that the defects are pure monovacancies, but rather are vacancies trapped by other defects, since such complexes may have significantly different electronic properties. Generally, one would also expect that vacancy complexes are more likely to be stable at high temperatures. The defect exhibiting the 287-ps lifetime is therefore a complex involving a single vacancy and some other defect species. Using the specific trapping rate of 10^{17} cm^{-3}/ns^{-1} estimated by Dannefaer, Mascher, and Kerr[18] for neutral vacancy-type defects in GaAs, the trapping rate of 0.7 ± 0.2 ns^{-1} suggests that the concentration of these complexes is $7\pm2\times10^{16}$ cm^{-3}.

In most samples, the carrier concentration is of the same magnitude or larger than the defect concentration, so the vacancies may be complexed with dopant impurity atoms. Samples 4, 5, and 6 have lower mobilities than the other undoped samples, and therefore may also contain impurities in concentrations comparable to that of the vacancy defects which may play a role in the formation of the complexes. However, it is also possible that the monovacancy complexes involve native defects such as antisites rather than impurity atoms. Measurements of the Doppler broadening of the annihilation radiation using a coincidence counting technique to reduce the background level are underway in order to investigate further the microscopic nature of these defects.

The defect lifetime of ~340 ps found in the very heavily doped n-type samples is close to the theoretically predicted divacancy lifetime of 347 ps,[15] suggesting that the open volume of the defects is comparable to that of a divacancy. The reduction in τ_2 at low temperatures suggests that the defects change their atomic configuration at low temperatures to appear more like a monovacancy. Configurational changes of defect complexes have been observed in many compound semiconductors, and are typically associated with varying degrees of lattice relaxation in the vicinity of the defect. The fact that the trapping rate is constant with decreasing temperature during this configurational change indicates that the defects are neutral.[17] The trapping rate of ~0.7 ns^{-1} therefore indicates that their concentration is also close to 10^{17} cm^{-3}.

It appears to be no coincidence that only the most heavily doped n-type samples show different defect characteristics, which would indicate that the large doping concentration might somehow be responsible for the anomalous positron lifetimes. There are several possible reasons why this may be the case.

The very large S and Sn dopant concentrations may lead to precipitate formation in concentrations sufficient to affect the positron lifetime characteristics. However, calculations of the solubility of Sn (Ref. 19) and S (Ref. 20) in InAs estimate the solubility limits to be in the 10^{20}- and 10^{21}-cm^{-3} ranges, respectively, so precipitate formation is unlikely. Even though we know only the carrier concentration, but not the actual dopant concentrations, in our samples, it is unlikely that concentrations of dopants sufficiently large for precipitate formation could be present. In the same vein, the dislocation densities in wafers 14–16, as determined through

EPD's, are on the low end of the range for our samples. This essentially rules out that dislocations and/or point defects associated with dislocations are responsible for the observed change in the defect characteristics.

Another possibility is that defects that are normally positively charged are neutral in samples 14, 15, and 16 due to the much higher Fermi energy, and therefore only trap positrons in these samples. Since most of the *n*-type samples are highly degenerate, calculation of the Fermi level position is not trivial. However, the Fermi level is clearly much higher in samples 14, 15, and 16 than in samples 12 and 13. It is therefore possible that the positron trap detected in samples 14–16 actually exists in all of the samples, but has a (+/0) level resonant with the conduction band.

A more likely explanation may be that the large dopant concentrations facilitate the formation of different defect complexes, especially if there is a saturation in the carrier concentration with increasing dopant concentration, as was observed in heavily Zn-doped InP.[13] Studies of Sn-doped bulk material[21] showed equal dopant and carrier concentrations up to 1.1×10^{19} cm^{-3}, and Sn- and Te-doped molecular-beam-epitaxy-grown material[22] showed no carrier concentration saturation up to 2.9×10^{19} cm^{-3}. However, discrepancies between the carrier concentration and total dopant concentration have been observed for dopant concentrations larger than 2×10^{19} cm^{-3} for bulk InAs:Te and $1–2\times10^{18}$ cm^{-3} for bulk InAs:S and InAs:Se.[23] In fact, the same authors performed precision density and lattice period measurements on these samples, and found a negative differential concentration of point defects, indicating the presence of vacancies. The concentration of vacancies was found to increase with the dopant concentration for S-, Se-, and Te-doped material, and was comparable in magnitude to the discrepancy between the dopant and carrier concentrations (10^{19}-cm^{-3} range). Although the vacancy concentrations measured in our samples are much lower, these results demonstrate that the formation of vacancy-type defects does correlate with a discrepancy between the dopant and carrier concentration in *n*-type InAs, as was also the case in *p*-type InP. Unfortunately, elastic recoil detection experiments on samples 12–16 to determine the actual S and Sn concentrations were inconclusive. The two main reasons are that (a) the sulfur concentrations are very near the detection limit of the technique, and (b) the Sn and In signals cannot be separated due to their proximity in the Periodic Table. For this reason, our suggestion that the observed changes in the defect characteristics might be triggered by ''overdoping'' should, at the present time, be treated as a plausible explanation. Further systematic work in this area clearly is necessary to establish the validity of the proposed mechanism.

V. CONCLUSION

A survey of InAs wafers has accurately determined the bulk lifetime of positrons in InAs to be 246 ± 2 ps. All wafers in this survey exhibit defect-related positron lifetimes. Most wafers contain $7\pm2\times10^{16}$ cm^{-3} of monovacancy complexes that have an associated positron lifetime of 287 ± 6 ps. In very heavily S- and Sn-doped *n*-type wafers, the open volume defects are larger, exhibiting a positron lifetime of 332–340 ps. This survey has established reliable experimental values for positron lifetimes in InAs, enabling the further study of the defect characteristics of this material using the positron lifetime spectroscopy technique.

ACKNOWLEDGMENTS

We are grateful to Robert Johnstone for performing the etch pit density measurements and to Dr. Jim Forster for the ERD analysis. This work was financially supported by the Natural Sciences and Engineering Research Council of Canada.

[1] L. F. Luo, R. Beresford, W. I. Wang, and H. Munekata, Appl. Phys. Lett. **55**, 789 (1989).
[2] J. F. Chen, L. Yang, M. C. Wu, S. N. G. Chu, and A. Y. Cho, J. Cryst. Growth **111**, 659 (1991).
[3] J. J. Pekarik, H. Kroemer, and J. H. English, J. Vac. Sci. Technol. B **10**, 1032 (1992).
[4] A. Kastalsky, V. J. Goldman, and J. H. Abeles, Appl. Phys. Lett. **59**, 2636 (1991).
[5] S. Dannefaer, J. Phys. C **15**, 599 (1982).
[6] V. N. Brudnyi, S. A. Vorobiev, and A. A. Tsoi, Phys. Status Solidi A **72**, 529 (1982).
[7] G. Dlubek and O. Brümmer, Ann. Phys. (Leipzig) **43**, 178 (1986).
[8] M. Misheva, G. Pasajov, G. Tubmev, and R. Yakimova, in *New Developments in Semiconductor Physics, Proceedings of the Third Summer School, Szeged, Hungary* (Springer-Verlag, Berlin, 1988), p. 232.
[9] L. Liszkay, L. Bottyán, and A. G. Balogh, Cryst. Prop. Prep. **12**, 199 (1987).
[10] H. C. Gatos and M. C. Lavine, J. Electrochem. Soc. **107**, 427 (1960).
[11] C. E. C. Wood, in *GaInAsP Alloy Semiconductors*, edited by T. P. Pearsall (Wiley, New York, 1982), p. 91.
[12] P. Kirkegaard, N. J. Pedersen, and M. Eldrup, *PATFIT-88: A Data-Processing System for Positron Annihilation Spectra on Mainframe and Personal Computers* (Risø National Laboratory, Roskilde, Denmark, 1989).
[13] J. Mahony, P. Mascher, and W. Puff, J. Appl. Phys. **80**, 2712 (1996).
[14] R. N. West, Adv. Phys. **22**, 263 (1973).
[15] M. J. Puska, S. Mäkinen, M. Manninen, and R. M. Nieminen, Phys. Rev. B **39**, 7666 (1989).
[16] M. J. Puska, J. Phys. Condens. Matter **1**, 7347 (1989).
[17] M. J. Puska and R. M. Nieminen, Rev. Mod. Phys. **66**, 841 (1994).
[18] S. Dannefaer, P. Mascher, and D. Kerr, J. Phys. Condens. Matter **1**, 3213 (1989).
[19] A. N. Morozov, V. T. Bublik, T. P. Grigor'eva, V. V. Karatev, and M. G. Mil'vidskii, Kristallografiya **30**, 548 (1985) [Sov. Phys. Crystallogr. **30**, 317 (1985)].
[20] L. D. Talis, V. V. Karataev, and M. G. Mil'vidskii, Inorg. Mater. **25**, 1362 (1990).
[21] V. T. Bublik, V. V. Karataev, M. G. Mil'vidskii, G. A. Nemtsova,

L. N. Perova, O. G. Stolyarov, and T. G. Yugova, Kristallografiya **24**, 1084 (1979) [Sov. Phys. Crystallogr. **24**, 621 (1979)].

[22] H. G. Lee, R. J. Fischer, L. C. Hopkins, and A. Y. Cho, J. Cryst. Growth **130**, 416 (1993).

[23] V. T. Bublik, V. V. Karataev, M. G. Mil'vidskii, G. A. Nemtsova, L. N. Perova, O. G. Stolyarov, and T. G. Yugova, Kristallografiya **24**, 528 (1979) [Sov. Phys. Crystallogr. **24**, 302 (1979)].